Bull. of Yamagata Univ., Nat. Sci., Vol. 20, No. 2, Feb. 2024

Sedimentary characteristics of event deposits overlying paleosols at the base of Mt. Chokai, Akita Prefecture, northeastern Japan: Exploring the potential for tsunami deposit

Tohru Yamanoi[1], Takeshi Saito[2], Fuyuki Tokanai[3],
Toru Moriya[3] and Susumu Konno[4]

Abstract

Event deposits have been discovered sandwiched between paleosols and dune sand at the base of Mt. Chokai along the Japan Sea coast in Akita Prefecture, Japan. These event deposits exhibit a diminishing thickness as they ascend the slope before ultimately disappearing. Their maximum elevation reaches 39.3 m on the slope. Radiocarbon dating of charcoal grains within these event deposits suggests an age of approximately 9,000 calBP. These deposits overlay paleosols that have experienced significant erosion, particularly at the lower portion of the slope. Erosional markings indicate a water flow directed toward the upslope. The majority of clastic materials within the event deposits originated from the paleosols, while some minerals were transported from the seaside. Additionally, a limited number of marine microfossils have been identified within the event deposits. A variety of sedimentary structures, including rip-up clasts, normal grading, suspension sedimentation, reversed grading, and fan delta structures, have been observed in the event deposits. Given the correspondence of many sedimentary facies within the event deposits with sequences observed in recent tsunami sediments, there is a possibility that these event deposits were formed by an ancient tsunami.

Key words : event deposits, paleosol, tsunami, dune sand, Japan Sea side

INTRODUCTION

Paleo-tsunami deposits have been extensively studied on the west coast of North America, where they are linked to earthquakes in the Cascade subduction zone, resulting in over 60 reported sites (Atwater et al., 1995; Peters et al., 2007, among others). In Japan, research on these deposits has primarily focused on the Pacific Ocean side due to the correlation between plate subduction and major seismic events (Goto et al., 2012; Sawai, 2017). Additionally, most paleo-tsunami deposit sites have been situated in coastal lowlands, such as lakes and marshes (Nanayama and Shigeno, 2004; Goto et al., 2012, etc.). This preference for coastal lowlands is attributed to their historical role as depositional sites with a high potential for continuous stratigraphic preservation, making them convenient locations for identifying non-ordinary tsunami deposits within the accumulated sediments (Sawai, 2012; Fujiwara, 2015, etc.). However, tsunamis can deposit sediments on various landforms, not limited to coastal lowlands, as they can intrude into diverse terrains (Minoura and Nakaya, 1991; Sugawara et al., 2008). Even when tsunamis reach slopes and leave deposits, the likelihood of these deposits

[1] Yamagata University (Professor Emeritus), Ueda 386-1544, Japan
[2] Faculty of Science & Technology, Meijo University, Nagoya 468-8502, Japan
[3] Faculty of Science, Yamagata University, Yamagata, 990-8560, Japan
[4] Department of Marine & Earth Sciences, Marine Works Japan Ltd., Yokosuka 237-0063, Japan

remaining intact is typically low unless they consist of large gravels, such as tsunami boulders (Goto, 2017). Nevertheless, there are instances where sediments persist on hillsides and high dunes, depending on the post-tsunami slope conditions (Bondevik et al., 2003; Minoura et al., 2013). Due to their association with massive tsunamis, these deposits, particularly their elevation data, hold significant value. The discovery of such tsunami deposits on slopes is crucial because it suggests the existence of geomorphic processes and soil-forming environmental "Sites" outside coastal lowlands that can preserve them (Hirakawa, 2014). In general, non-ordinary sediments formed in a short time in ordinary sediments were called "Event deposits" by Shiki (1988). The author has identified several Event deposits on the slopes of the Shonai dune, indicating the occurrence of two major tsunamis between the 8-9th and 10-11th centuries (Minoura et al., 2015; Yamanoi et al., 2016). In these cases, our attention is drawn to the fact that the Event deposits on paleosol slopes were extensively covered by dune sand. This rapid sand deposition occurred immediately after the tsunami event, effectively preserving the sediment. Furthermore, significant tsunamis are typically associated with large earthquakes, which often follow a periodicity. Earthquakes on the Japan Sea side differ from those related to the subduction zone on the Pacific side and are instead a result of the active geological structure along the eastern margin of the Japan Sea (Okamura et al., 1998, etc.). The large tsunami deposits found on the Shonai dune were probably caused by tectonic movements in the "Sakata-oki Uplift zone" (Okamura et al., 1998), which is near the coast (Yamanoi et al., 2016). In areas where such massive tsunamis have occurred, there is a possibility of finding new deposits by investigating sites where they have been preserved, as mentioned earlier. With this background, our focus has shifted to paleosols in Akita Prefecture, just north of the Shonai area, which lies along the coast of the Sakata-oki Uplift zone (Fig. 1, left). We specifically searched for locations where wind-blown sand has covered these paleosols. As a result, Event deposits were discovered on a coastal hill (elevation 36-39 m) at the base of Mt. Chokai in the southern part of Akita Prefecture (Figs. 2 and 3). If this sediment is indeed the result of a tsunami, it is believed to be a massive tsunami. However, because there is limited information on tsunamis of similar size in modern tsunami studies, it's challenging to confirm these event layers as tsunami deposits. Therefore, this study aims to investigate the depositional environment of these Event deposits from various angles and explore their potential as indicators of past tsunami activity.

MATERIALS AND METHODS

1. Field survey

We conducted a field survey focusing on paleosols in Akita Prefecture, located to the north of the Shonai area, with an emphasis on the wind-blown sand that covers them. This region, situated at the base of the Chokai volcano, is characterized by rocky beaches and the absence of coastal dunes. However, Event deposits were discovered behind areas where small sandy beaches had formed.

The Event deposits were widely exposed including their surroundings, and then thinly scraped smooth surfaces were observed. To determine the elevation of the Event layer, measurements were taken using a Total Station from a benchmark point along Route 7 National Highway, located approximately 500 m southwest of the outcrop (see Fig. 2). The topography of the surrounding area was delineated by aerial photo-reading, followed by a topographic and geologic survey.

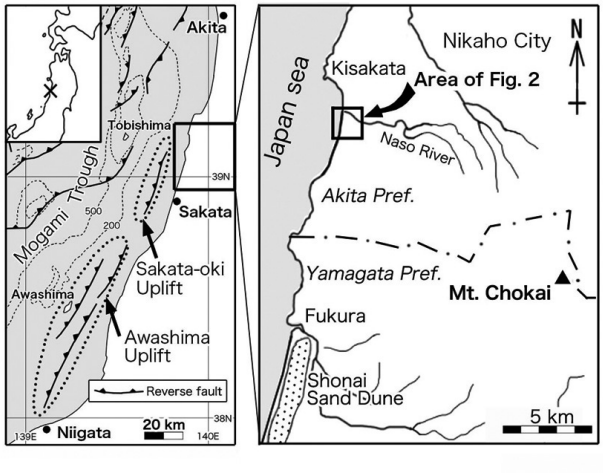

Fig. 1. Guide maps for the study area. The left panel shows the tectonic structure modified by Okamura et al. (1998).

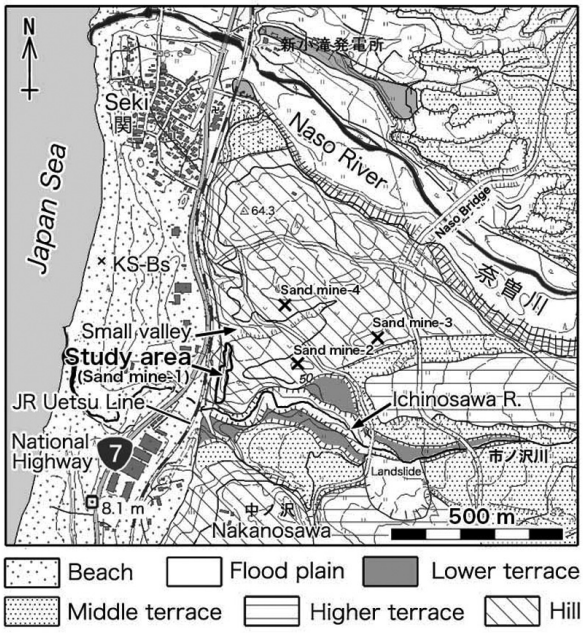

Fig. 2. Location map of the study area (sand mine-1) where the Event deposits were found and the neighboring topography. Geographical maps adapted from the Digital Japan Web System of the Geospatial Information Authority of Japan.

2. Sample analysis

For radiocarbon dating, samples of carbonized material (burnt charcoal) from the Event deposits and the uppermost layer of the

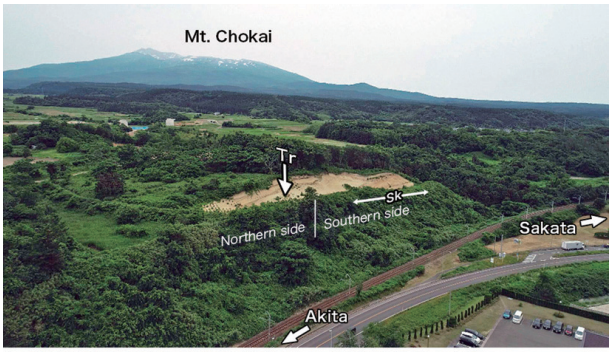

Fig. 3. Bird-view photograph around the study area was taken by the drone.(Sk): Extent of the sketch (Fig. 4), (Tr): Trench point (Fig. 8).

Paleosol just below the Event deposits were utilized. These samples underwent ultrasonic cleaning (in pure water and acetone), followed by treatment with the acid-alkali-acid (AAA) method and subsequent graphitization at the Analysis of Mass facility at Yamagata University's High Sensitivity Accelerator Center, employing an AMS system (YU-AMS: NEC 1.5SDH). The resulting ^{14}C concentrations were calibrated using OxCal 4.3 (IntCal 13) after correction for isotope fractionation effects.

Particle size analysis was performed by dispersing the samples in a 0.1 wt% sodium hexametaphosphate solution for 2 minutes using an ultrasonic homogenizer (US-150T, Nippon Seiki Mfg. Co., Ltd.). Wet measurements were then carried out using a laser diffraction and scattering particle size analyzer (MT3300, MicrotracBEL), with the refractive index set to 1.81 (performed at the Akita Industrial Technology Center).

Organic particles were subjected to humin analysis, referred to as "palynodebris," due to their insolubility in acid and alkaline solutions. This analysis followed the pollen analysis method and involved the concentration of pollen particles (10-200 μm fraction) through a series of treatments: KOH solution, HF, acetolysis, and heavy zinc chloride solution, with rinsing between each step. However, the

treatments for micro charcoal content analysis excluded the HF and acetolysis procedures used in the above method.

Microfossils (diatoms) were analyzed from samples (approximately 10 g each) following the method outlined by Akiba et al. (1982). Additionally, siliceous fossils were separately collected using the phytolith concentration method. In this method, approximately 12 g of each sample was dried, passed through a 250 μm mesh, boiled in hydrogen peroxide, had its fine-grained clay content removed through sedimentation, was separated in SPT heavy liquid with a specific gravity of about 2.4, and then the emergent portion was washed and sealed.

Mineral analysis was conducted according to the procedure described by Ikuta et al. (2016). Particles within the 1/8 - 1/16 mm size range, sifted in water, were examined, and the mineral composition was divided into all particles and heavy minerals, respectively. Additionally, the refractive index of volcanic glass was measured.

RESULTS

1. Geology and topography

The study area is a coastal hillside south of Seki, Kisakata-cho, Nikaho City, Akita Prefecture. The ground surface in this area consists mainly of medium-grained sand and the only outcrop is a Sand mine. The four Sand mines in this area are shown in Fig. 2. Except for Sand mine-4, loamy beds were exposed under the sand layer. In Sand mine-2 and 3, medium-grained sand overlies the loamy layer with a clear boundary. In Sand mine-1, the Event layer was found between the loamy layer and the medium-grained sand layer. This outcrop is the closest to the sea, located on a steep cliff, and is clearly visible from National Highway 7 (Fig. 2). A drone photo of the outcrop from the northwest is shown in Fig. 3. The medium-grained sand layer is a Dune sand made of wind-blown sand since the development of compound cross laminae is remarkable. The geology of this hill is the Pleistocene Nishime Formation overlying the Neogene System in a harmonic structure, which is covered by Paleo-dune deposits (Ozawa et al., 1982). The Paleo-dune deposits are overlain by the Kisakata mudflow deposits (about 3,000 years ago), which created the hummocky hill of the Kisakata in the northern part of this site. The ^{14}C age of the humic sand layer 2 m below the Kisakata mudflow deposit is 7700 ± 210 years BP (Gak-7096) (Ozawa et al., 1982). Since the Event layer here is located just below the lowest level of the strata considered to be Paleo-dune deposits, it is expected to have been formed at an earlier age than the above age.

The topography of this area can be roughly divided into low land, river terrace and hill (Fig. 2). The low land is further divided into beach and flood plain. The river terrace is divided into three categories according to the relative heights: Higher terrace (>30 m), Middle terrace(20 m ±), and Lower terrace (< 10 m). The hill is higher than the Higher terrae and has undulating slopes (Fig. 2). The Ichinosawa River, close to the south of this site, has been eroding downward, and the strata below the Lower terrace surface can be observed in a continuous sequence. In the outcrops here, from the lowest level, there are fine-grained tuff breccia: the Nishime Formation (15 m to 17 m El.), old riverbed gravel (17-18 m El.), loamy soil (40-50 cm thick), and black soil (40-50 cm thick) at the uppermost level. The surface elevation of the Lower terrace here is 19 m. On the other hand, to the north of the site, there is a small valley (hereafter called "Small valley") with terraced rice paddies (Fig. 2).

2. Observations of the Event deposits

The distribution area of the Event layer is divided into the Southern side, which is

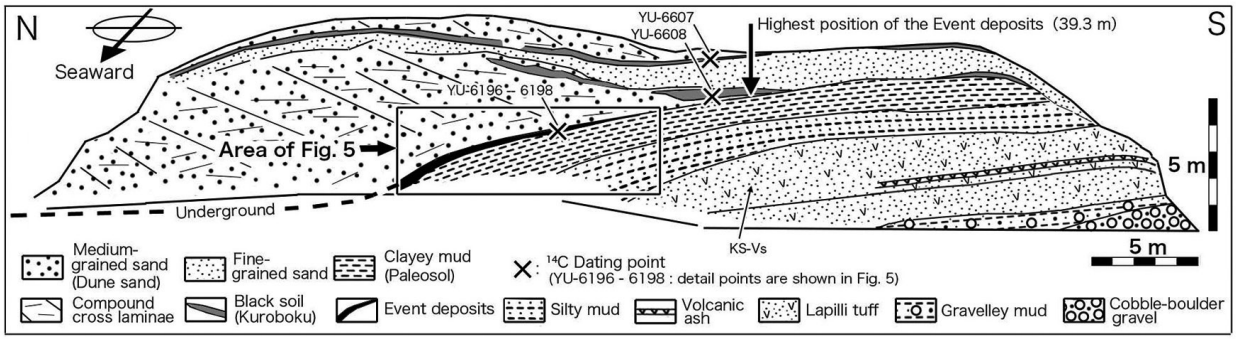

Fig. 4. Sketch of the Southern side of the outcrop for the geologic profile.

exposed on the slope, and the Northern side, which is shallowly buried below the outcrop (Fig, 3).

2.1 Southern side

On the Southern side, the Event layer and its above and below are well observed. A cross-sectional sketch in the direction of the coastline is shown in Fig. 4. The lowest part is a sandy gravel bed composed mainly of large, rounded gravels, which changes upward to a loam layer interbedded with gravels. Above them is a hard fine sandy volcanic ash (lapilli tuff) interbedded with gray-colored volcanic ash. And its upper layers are silty and clayey mud. The Event layer covers the uppermost part of the clayey layer and is almost continuous within the rectangular box in Fig. 4, but it becomes thinner and more interrupted at higher elevations. The Event layer is covered by well-sorted medium-grained sand. The distribution of the Event layer is shown in Fig. 5 in cross-section (horizontal: vertical = 1:2). The lithology of the Southern side is described below, and the soil color is shown in parentheses as the standard Munsell color of wet soil. Since the morphology and lithology of the Event deposits change depending on the distribution elevation, the slope is classified as "Lower section"(< 37 m El.) , "Middle section"(37-38 m El.), and "Higher section" (> 38 m El.) (Fig.5). There is a massive "Clayey mud" just below the Event deposits. The upper part is brown-gray to gray-brown (7.5YR5/1-7.5YR5/2), and the lower part is orange-brown (7.5YR7/6-7.5YR4/6), and there is a gradual transition zone of 5-10 cm between the two layers. As described later, this Clayey mud is derived from Paleosol (Ps), which can be divided into "Dark brown colored Paleosol " (Dp) in the upper part and " Brown colored Paleosol " (Bp) in the lower part. The Event deposits cover the (Bp) in the Lower section and the (Dp) in the Higher section (Fig. 5) . The thickness of the Event layer is 30-20 cm in the Lower section (around Fig. 5A), and it becomes thinner in the Middle section (around Fig. 5C) with irregular changes, and then discontinuously breaks off in the Higher section (around Fig. 5D). However, the highest part of the Event layers (right outer part of Fig. 5) continues as scattered gray silt blocks (irregular cross-sections with indistinct contours), which are visible up to 39.3 m elevations when carefully traced (Fig. 4). On the other hand, the Event layer in the Lower section (the leftmost layer in Fig. 5) is buried in the subsurface on the Northern side, and its approximate location is indicated by the coloring of the buried soil by groundwater seeping from the upper surface of the Event layer (Fig. 4). The buried Event layer is found to be almost horizontally distributed on the Northern side. Typical cross-sections of the Event deposits are shown in Fig. 5 (A, B, C, and D), and the most schematic part (point E in Fig. 5) is shown in Fig. 6. Many

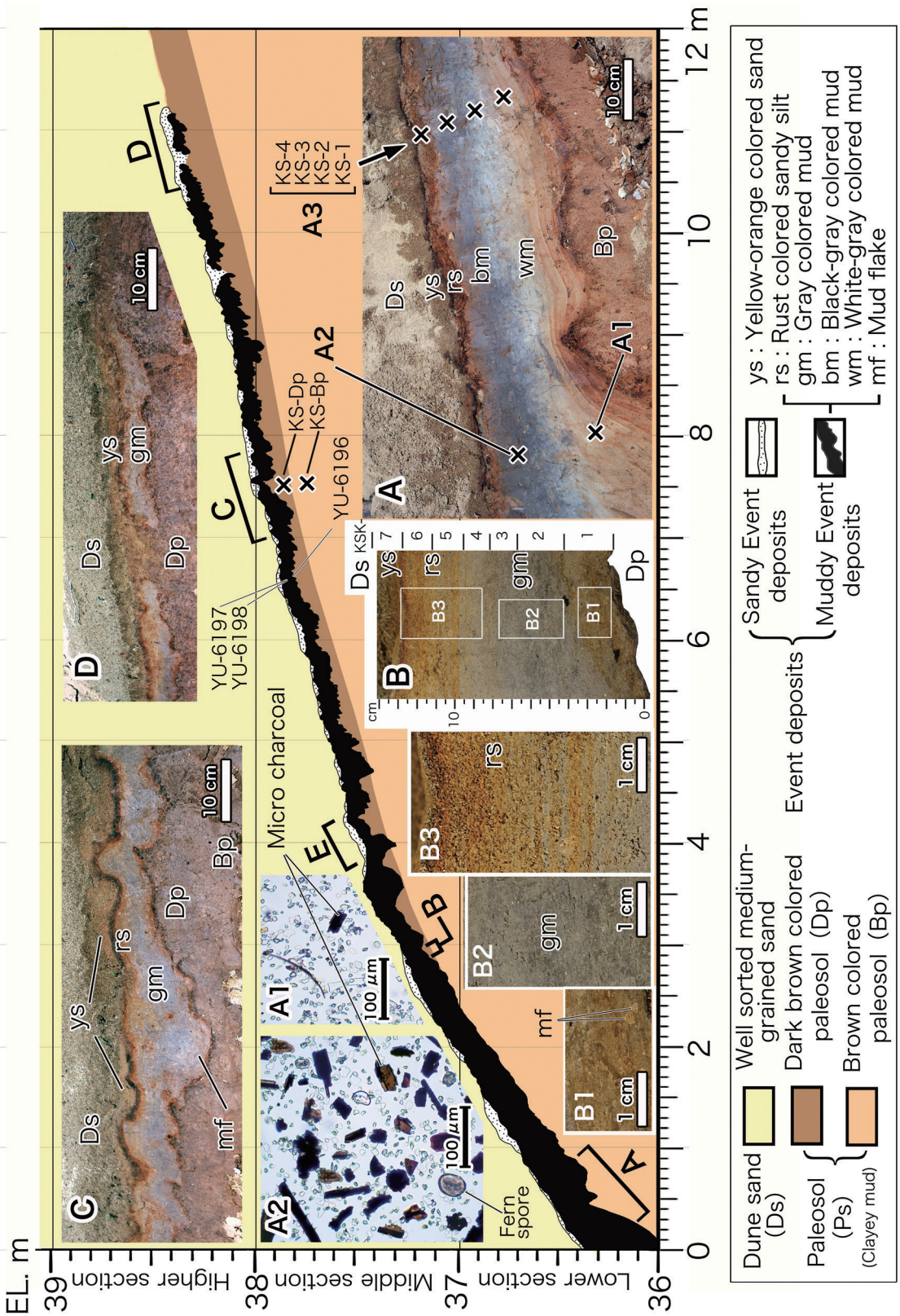

Fig. 5. Section of the Event deposits and their photographs. The extent of each photograph indicates in the slope section. Sample positions for a grain size analysis are shown beside the (B) picture. (A1, A2): Micro charcoal of the (wm) and (bm) in the (A) part, (KS-Dp, Bp, and A3): Sample positions for analyses of a palynodebris and mineral composition, (B1-B3): Close-up pictures in the (B) part, (E): Extent of Fig. 6.

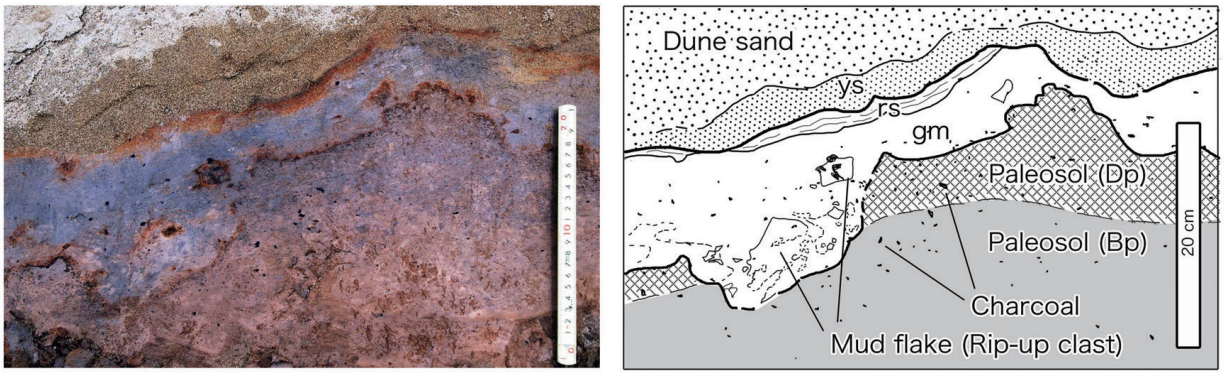

Fig. 6. Photograph and sketch of the Event deposits at the (E) point in Fig. 5. (gm): Gray colored mud, (rs): Rust colored sandy silt, (ys): Yellow-orange colored sand.

irregularities are observed on the bottom of the Event layer (Figs. 5, 6). The unevenness is rather smooth in the Lower section but noticeable in the Middle and Higher sections (Fig. 5). These concavities are erosional marks, which will be described later. Their V- or U-shaped cross-sections tend to tilt upward on the slope in the Middle section (Fig. 5C, left), but less so in the Higher section (Fig. 5D). This tendency can be measured as the angle between the central axis of the erosional mark and the slope (θ : axis angle of the erosional mark). The shape of the erosional mark and its handling method is described in Yumi and Ishihara (2012), and measurements were made on the Middle and Higher sections for erosional marks with a length of 5-10 cm. These results are shown in Fig. 7, together with the method of measurement. The Fig. shows that the erosional mark tends to be tilted upward ($\theta > 90°$) in the Middle section (Fig. 7, lower left), while its axis does not tend to be concentrated in a specific direction in the Higher section (Fig. 7, lower right). The Event deposits consist of "Muddy Event deposits", which form the main body, and thin "Sandy Event deposits" that cover it discontinuously. The Muddy Event deposits show "white-black layer differentiation" in the Lower section, which is divided into "White-gray colored mud (wm)" (5Y8/1-5B6/1) in the lower part and "black mud (bm)" (5B5/1-5B3/1) in the upper part (Fig. 5A). At this location, samples of the (wm) and (bm) (Figs. 5A, A1, A2) were collected and the content of micro charcoal was compared. The proportion of micro charcoal among all inorganic particles was 18% in the (bm) and 3% in the (wm). Then the black mud (bm) clearly contained many micro charcoals (Figs. 5A1, A2). The (wm) and (bm) of the Event deposits disappear as the (wm) thinned toward the slope higher, and only (bm) becomes in the middle of the (A) and (B), and further up, the color of the (bm) gradually changes to gray (5Y5/1) and shifts to "Gray-colored mud (gm)" (Figs. 5B, 5C, 5D). The lower part of (gm) contains "Mud flakes (mf)" of the same lithofacies as the (Dp), either in the form of conglomerates or irregularly shaped. This (mf) is often found in the concave bottom of the (gm). In addition, the (mf) is not completely separated from the (Dp) (Figs. 5C, 6).

Muddy Event deposits and the upper parts of the (Dp) and (Bp) contain many charcoals (the largest one about 2 cm in length) (Fig. 6). The Muddy Event deposits have weak parallel laminations at the top and bottom of them. These are highlighted by rust-colored coloration. The lower lamination has no visible differences other than coloration (Fig. 5A). In contrast, in the upper lamination, dense

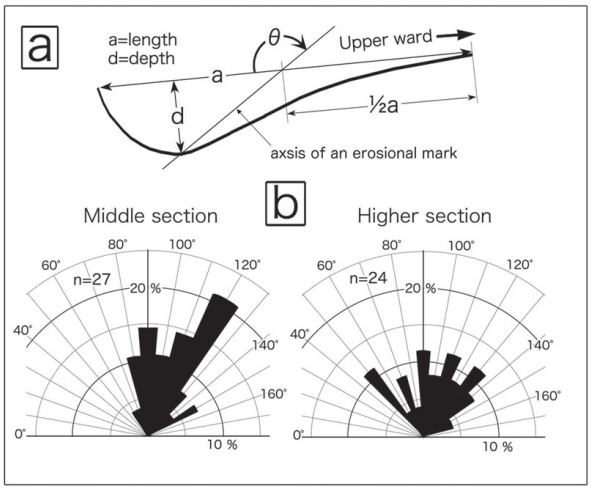

Fig. 7. Tilt angle(θ) of an axis of the erosional mark on the paleosol. (a) Schematic geometry of an erosional mark. (b) Frequency diagrams of the tilt angle (θ).

and sparse sand grains are colored rust and gray, respectively (Fig. 5B3). The lamina of the upper part of the Muddy Event deposits is not clear in some parts. In some cases, the lamina is hardened by the deposition of iron oxide (lignite) in the lamina. The upper part of the Muddy Event deposit is classified as "Rust-colored sandy silt (rs)" (5YR5/8-3/6) because it is colored by being generally sandy with or without lamina (Figs. 5, 6). This (rs) is progressively related to the lower (bm) and (gm) but has a clear boundary with the upper Sandy Event deposits. The Sandy Event deposits are classified as "Yellow-orange colored sand (ys)" because it consists of yellowish-orange clay and silty sand (10YR7/6), which is lighter in color than the medium-grained Dune sand (Ds) (10YR5/2) that covers it. The (ys) is thin, often less than 5 cm, and thicker when the top surface of the Muddy Event layer is concave.

2.2 Northern side

The Northern side is an outcrop incised about 10 m landward from the Southern side (Fig. 3, Northern side of Fig.4). The lower part of the outcrop was excavated at intervals of a few meters. The Event deposits were observed to be 40-50 cm thick covering the (Bp), covered by well-sorted medium-grained sand (Ds), and distributed almost horizontally (Fig. 8). After this exploration, we excavated a trench point about 2 m from the seaside to landward where a thick (ys) was observed on the Muddy Event deposits (Figs. 3 and 8: Trench point). The cross-section is shown in Fig. 9. Here, the well-developed (ys) covers the Muddy Event deposits (dip is about 5° seaside). From the (ys1) to (ys3) as a unit of (ys) cover the top of (rs) from the landward to the seaward in order with a downlap structure. The medium-grained sand in each unit of (ys) shows a change to fine-grained sand in the upper part and silty sand in the top part, so each unit shows normal grading (Fig. 9).

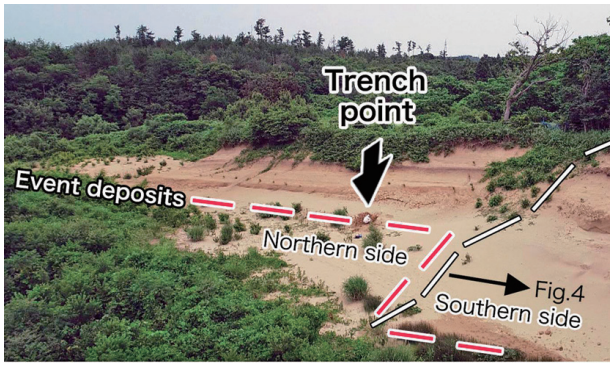

Fig. 8. The northern side of the outcrop where the Event deposits are distributed underground almost horizontally in the coastline direction.

2.3 Grain size

Event deposits were cut off from point (B) of the Middle section (Fig. 5) as a sample for detailed observation of grain size composition. The surface of the deposits was further shaved with a sharp knife in a room and observed. The results show that this part can be divided into three parts based on the characteristics of grain size composition. The lowest part (B1) is composed of "Mud flake (mf)" particles of the same lithofacies as those in the Paleosol (Ps) scattered in the muddy substrate as cross-sectional particles with sizes smaller than 3 mm (Fig. 5, B1). The middle part (B2)

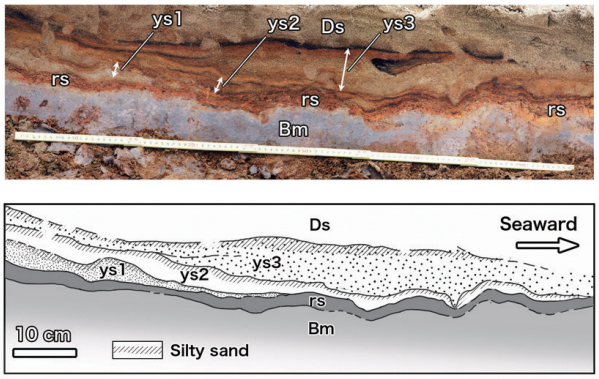

Fig. 9. Photograph and sketch of the Sandy Event deposits (ys: ys1, ys2, and ys3) observed at the trench point (Fig. 8), showing a downlap deposition toward the seaward on the top of the rust-colored sandy silt (rs). (Bm): Black colored mud, (Ds): Dune sand.

is mostly muddy (clay-silt) (Fig. 5, B2). The upper part (B3) shows a lamination with finely alternating muddy and sandy portions and an inverse grading to a sandy part (rs) (Fig. 5, B3). The above-observed Muddy event deposits (gm, rs) were divided into 6 parts, and the Sandy event deposits (ys) at the top, (Dp) just below the event layer, and (Ds) just above the event layer were added, and a total of 9 samples (Fig. 5, B) were measured using a grain size analyzer. The results are shown in Fig. 10. The grain size change in the Event layer above KSK-3 shows a tendency toward inverse grading.

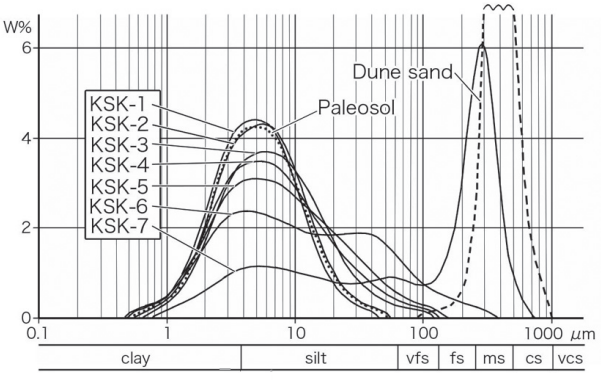

Fig. 10. Grain size distribution of the Event deposits located at the (B) point of Fig. 5.

2.4 Dating

Samples for ^{14}C dating were collected from the three points marked with × in Fig. 4. The upper two samples (bottom: YU-6608, top: YU-6607) are the lower portions of the black soil (Kuroboku) sandwiched between the upper Dune sand layers of the Event deposits. It is necessary to examine what to select as the organic matter sample of an event layer (Sawai, 2012). Grass seeds and leaves were suitable for the Event deposits of the Shonai dune (Yamanoi et al., 2016), but the Event layer here is significantly decomposed by plant remains and could not find suitable charcoal materials. The next best samples are three kinds of charcoals: the uppermost part of Paleosol just below the Event deposits (YU-6196), burned charcoal in the Event deposits (YU-6197), and a small black mass surrounded by brown limonite in the Event deposits (YU-6198) (Fig. 4). The results of these measurements, together with those of the upper stratigraphic levels of the Dune sands, are shown in Table 1.

2.5 Palynodebris

Palynodebris analysis was performed on the Paleosol (2 levels) at the site (C) and the Muddy Event deposits (4 levels) at the site (A), (A3 in Fig. 5). These samples are representative of the respective lithologies (KS-1: wm, KS-2: wm/bm gradient, KS-3: bm, KS-4: rs). Palynodebris is a humic substance insoluble in acid and alkaline solutions. Here we refer to particles of biogenic origin that are observed under the microscope as organic residues by the pollen analysis method. These particles at this site are broadly classified as "Palynomorphs", which are pollen and spores that leave the organism or its organs, "Micro charcoal", which are particles of burning charcoal, and "Rod-shaped organic matter", which cannot be identified. Palynomorphs were further classified into "Pollen," "Fern spore," "Fungi spore," and "Acritarch" of unknown affiliation. The Micro charcoal is a

Table 1 Radiocarbon ages obtained from the Event deposits and the upper two black soil layers.

Code No.	Sample material	$\delta^{13}C$ (‰)	^{14}C Age (yrBP±1σ))	Calibrated Age (yrBP) 1σ	2σ
YU-6196	Top of the Paleosol	-20.16±0.24	8742±27	9770 (61.8%) 9654 9648 (6.4%) 9630	9889 (95.4%) 9596
YU-6197	Charcoal in the Event deposits	-26.96±0.29	8341±26	9430 (26.2%) 9397 9380 (2.7%) 9376 9362 (39.4%) 9310	9448 (95.4%) 9291
YU-6198	Black pebble coated by limonite in the Event deposits	-21.35±0.27	8782±30	9888 (20.3%) 9840 9825 (41.7%) 9732 9721 (6.2%) 9706	9907 (95.4%) 9686
YU-6608	Lower black sand (kuroboku)	-24.97±0.18	6309±24	7269 (56.5%) 7242 7214 (31.7%) 7179	7276 (95.4%) 7169
YU-6607	Upper black sand (kuroboku)	-22.39±0.18	2515±20	2723 (18.6%) 2700 2634 (12.6%) 2618 2589 (33.2%) 2540 2527 (3.8%) 2520	2736 (26.2%) 2686 2639 (15.6%) 2613 2597 (53.7%) 2497

blackish brown, roughly quadrilateral (plate-like in three dimensions) burning charcoal particle that retains organic structure, although the source plant cannot be identified. These are classified as "Rectangular type" and "Square type". The criteria for distinguishing between the two types are as follows: Rectangular type is defined as having a long side/short side of 2 or more, and Square type is defined as having a long side/short side of less than 2. The more prolific is the elongated, banded (flattened bar-shaped in three dimensions), black opaque organisms. Although the affiliation of this Rod-shaped organic matter is unknown, it is the main particle of the palynodebris at this site, so we have specifically designated it as "Black Rod". A representative example of such palynodebris is shown in Fig. 11a and its composition in Fig. 12a (n=1000). The compositional change of the palynodebris in the Muddy Event deposits, which was more than 90% in Black Rod in KS-1, is decreasing to the upper part. Micro charcoal and Palynomorphs are increasing in the upper part. For Black Rods among the palynodebris, the lengths of the long and short sides were measured for each 50-500 μm long fraction (n=100). The results are shown as line and bar graphs of the size distribution of the particles in terms of long length and cross-sectional area (optical section in microscopy: long length × short length), respectively (Fig. 12b). From this figure, it is observed that both size length and area tend to decrease toward the upper. This trend is more evident when combined with the composition of the

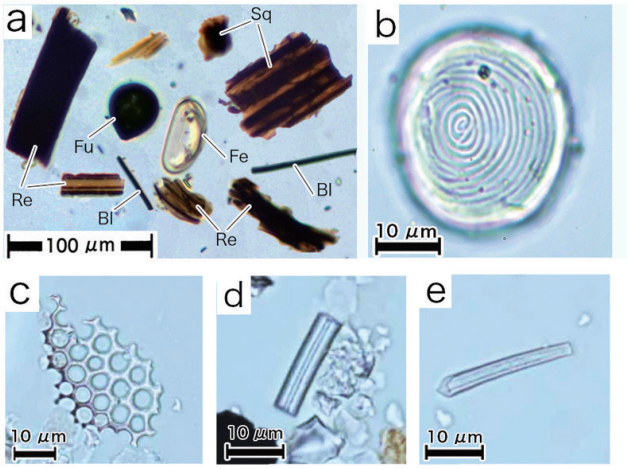

Fig.11. Micrographs showing some microfossils occurred from the Event deposits (KS-3).(a) Some representative types of palynodebris, (Fe): Fern spore, (Fu): Fungi spore, (Sq): Square type of a micro-charcoal, (Re): Rectangular type of a micro-charcoal, (Bl): "Black Rod" (rod-shaped organic matter). (b) *Concentricystes*, classified morphologically as an acritarch which is an indicator of the shallow freshwater condition. (c) Fragment of a diatom (Centrales) or Radiolaria, (d-e) Sponge spicule.

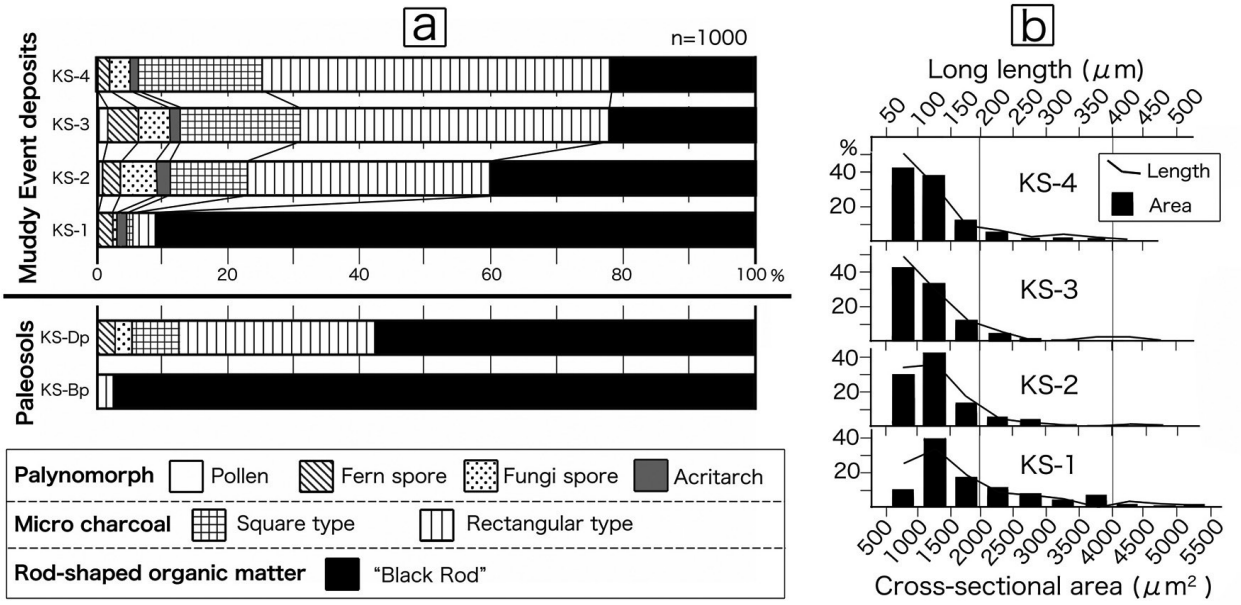

Fig. 12. Diagrams of compositions of the organic particles in the Event deposits and the Paleosols. (a) Components of the palynodebris of the Paleosols and the Event deposits. (b) Size distribution of the "Black Rod" of the muddy Event deposits.

Black Rod of the palynodebris (Fig. 12b). The composition of Acritarch of the palynodebris was determined separately by morphological subdivision (n=100). Of these, *Concentricystes* (Fig. 11b), described later, was not occur from the Paleosols, but KS-1 to KS-4d occurred in 2, 10, 7, and 10%, in that order. Microfossils (diatom) were analyzed in seven Muddy Event deposits (Fig. 5, B) and three Sandy Event deposits (Fig. 9, ys1-3) of the same sedimentary level as the grain size analysis, including Paleosols. No microfossils were observed in these samples. To further increase the concentration of siliceous fossils, the same stratigraphic levels (KS-Bp, Dp, 1, 2, 3, 4) and Dune sand (Ds) samples (Fig. 5) were analyzed by the aforementioned phytolith concentration method. Among them, diatom (Centrales) or radiolarian debris (Fig. 11c) and sponge spicule (Fig. 11d, e) was found in small quantities only from KS-3.

2.6 Mineral composition

Mineral analysis was performed on the following 9 samples. They are 6 samples of the same sedimentary level as the palynodebris analysis, in addition to the Sandy Event layer (ys2) (Fig. 9), volcanic deposits of Mt. Chokai (Lapilli tuff) (Fig. 4) of the underlying Paleosol Formation, and the present beach sand (Fig. 2). The analysis includes all particle composition (n=200), heavy mineral composition (n=200), morphological classification of volcanic glass, and refractive index measurement of volcanic glass. The results of the analysis of all particles and heavy minerals are shown in Fig. 13. The refractive indices of the volcanic glasses were measured in four stratigraphic levels (n=60): Paleosols (KS-Bp, Dp) and lower Event deposits (KS-1, 2), where the content of the volcanic glass is relatively high. The refractive indices ranged from 1.4976 to 1.5101, with a mode of 1.502 for all four samples.

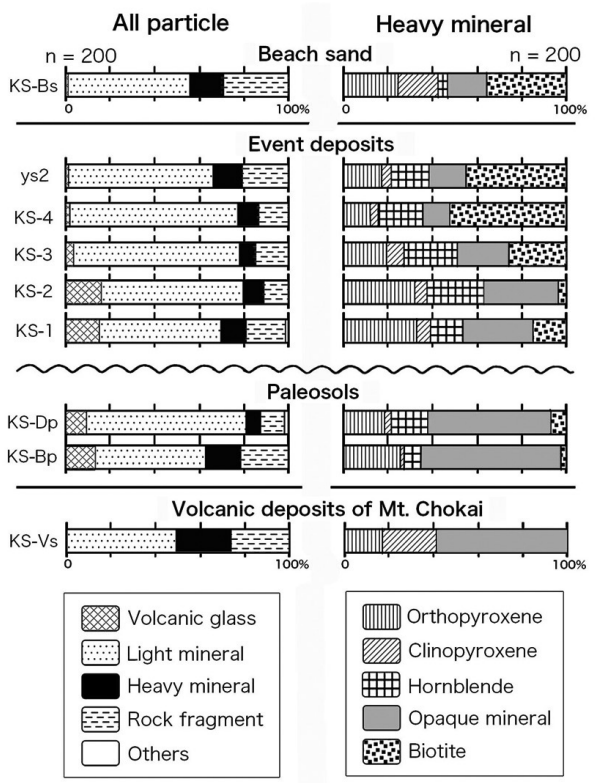

Fig. 13. Mineral compositions of the Event deposits, basement soils(Paleosols), volcanic deposits, and beach sand.

DISCUSSION

1. Sedimentary environments

As shown in Fig. 4, the lowest part of the outcrop consists of a clast-supported, rounded cobble-boulder gravel layer, which represents a fluvial deposit. Above this gravelly layer, there is a layer of gravelly mud with a loamy matrix, representing aeolian deposits filled with gravels. These gravels became exposed on the ground surface after the riverbed turned into dry land. The Lapilli tuff layer, over 3 m thick, contains a thin layer of volcanic ash deposited from the nearby Chokai volcano. Above the pyroclastics, there are layers of silty mud and clayey mud, which represent aeolian deposits on dry land. The clayey mud deposits are considered loess due to their median grain size of 4.9 μm (see Paleosol in Fig. 10), which falls within the range of typical loess grain sizes (3-20 μm) originating from the continent (Naruse & Inoue, 1982; Naruse, 2006). These loess deposits also exhibit paleosol characteristics, having once been at the surface and undergone soil formation (Yamanoi, 2015). The Event deposits overlay this Paleosol and are covered with well-sorted, medium-grained sand, which acts as a protective layer. This sand layer is dune sand composed of wind-blown sand, which is also found further inland (Ozawa et al., 1982). A layer of black soil (known as Kuroboku) is sandwiched between the upper part of the sand layer at this site. The dip of the stratum below the Event layer indicates the inclination of the aeolian deposits, parallel to the slope at that time.

The ages of the Event deposits are more recent than the ^{14}C age of the Paleosol (9,889-9,596 calBP) and are close to the age of burned charcoal found within the Event deposits (9,449-9,291 calBP). However, considering that this age includes time for transport and deposition after plant burning, the age of the Event layer is estimated to be around 9,000 years ago, placing it in the Early Jomon Period of Japanese prehistory. The presence of burnt charcoal and micro charcoal deposition is indicative of Jomon people (Yamanoi, 1996), and there is a Jomon Period archaeological site located to the south of the survey site (Akita Prefectural Board of Education, 1991).

2. Narrowing down the origin

The upper part of this Event layer exhibits parallel laminations with a fine repetition of mud and sand layers. Its upper section also displays inverse gradations that transition into sand layers, indicating hydrogenous sediments (Fig. 5B3). Since the sediments found consistently at this hillside site are wind-formed, the abrupt appearance of hydrogenous sediments can be attributed to Event deposits, as proposed by Shiki (1988). Given the gradual lateral change in lithofacies of the Event layer,

it can be inferred that a water body existed continuously for a significant duration.

The site is situated on a hillside surrounded by cliffs on the south and seaside, with a slope leading to the Small valley on the north side (Figs. 2 and 3). In such a location, the following water-related events could potentially lead to hydrogenous deposition: floods, mudflows, debris flows, springs, snowmelt water, liquefaction eruptions, lakes, storm surges, and tsunamis. Below is an evaluation of whether these water-related events could have deposited materials at this site.

The first question pertains to whether the Event deposits at an elevation of 36 m or higher are flood deposits from around 9,000 years ago. In general, during the early Holocene, riverbeds were typically situated near the Lower terrace face. The Naso River to the north and the Ichinosawa River to the south are rivers that might have caused flooding at this site. Fig. 2 shows terraces with relative heights of 10 m or less formed by both rivers. A common feature observed at the uppermost part of these Lower terraces and the Ichinosawa River is a layer of black soil covering the old riverbed gravels. Most of this black soil is younger than 10,000 years (Yamanoi, 1996). The Paleosol (Dp) just beneath the Event layer contains micro charcoal, indicating the beginning of black soil formation (Kuroboku). This timing corresponds with the commencement of black soil (aeolian deposits) deposition on the old riverbed gravels (18m EL.) of the Ichinosawa River. Consequently, at the time of Event deposit formation, the riverbed elevation of the Ichinosawa River was below 18 m. While floods from the Ichinosawa River might have occurred at this riverbed elevation, they wouldn't have reached the Event deposits at 36-39 m EL., which are higher than 18 m (Fig. 2). Flooding in the Small valley on the north side is unlikely because it is a narrow catchment area on the hillside with low water volume. Conversely, if the Naso River flowed into this valley, it originated from the upper reaches (60 m EL.) southwest of the Naso Bridge (Fig. 2). The relative heights here are approximately 30 m, so even if the riverbed of the Naso River at the time of the event was about 10 m higher than the Lower terrace surface, it would still be more than 20 m higher. Therefore, it is improbable that the Naso River flooded from the upper reaches of the Small valley during that period. Consequently, it can be concluded that the formation of the Event layer was not caused by floods from either the Ichinosawa River, the Small valley, or the Naso River.

Next, with regard to mudflows and debris flows, given that this site is located at the base of the Chokai volcano, mudflows would likely have occurred on the slopes near the summit (Ozawa et al., 1982), and debris flows would also have been frequent. It's also possible that the rupture of a lake or swamp at the base of the volcano could have triggered a mudflow-like event. However, all these flows move downhill from their points of origin, and mudflows and debris flows from the hinterland would have flowed through the old river site (Middle or Lower terrace surface), which is lower in elevation compared to the hillside outcrop (Fig. 2). Consequently, it is unlikely that mudflows and debris flows would have reached this particular point.

Additionally, spring water, snowmelt, or heavy rainfall could have caused slope runoff. Nevertheless, since the Event layer is situated near the top of the slope (Figs. 3 and 4), the water supply from these sources would have been limited, and the steepness of the slope would not have allowed for significant water accumulation. Therefore, the likelihood of forming a muddy layer under these circumstances is very low. If a lake were to form, it would have been due to the damming of the Small valley. However, the occurrence of a dam that raises the water level above the elevation of the Event deposits, in other

words, a mass of soil blocking the valley due to slope failure, is topographically implausible, and there is no evidence supporting the existence of such a dam.

Muddy deposits resulting from water eruptions due to liquefaction are also a possibility. Liquefaction occurs when pore-fluid pressure increases due to seismic motion in coarse-grained ground like sand, provided there are loosely deposited sandy sediments and groundwater to fill them (Tohno, 2000). At that time, there are 2-3 m of clayey and silty deposits below the surface, beneath which lies a Lapilli tuff layer. The Lapilli tuff is composed of fine sand-gravel-sized particles filled with volcanic ash and does not constitute a loosely sedimentary deposit with advanced cementation. Furthermore, the Lapilli tuff does not contain groundwater because it slopes from the hill's summit to the Small valley (Fig. 4). Consequently, liquefaction would not have occurred here at that time.

Regarding storm surges (tidal waves), this phenomenon is primarily observed in Japan's gulf coast areas during typhoons (Kuronuma, 1970). Since this area is situated on the Japan Sea side and does not form a bay shape, the possibility of large-scale storm surge (tidal wave) occurrence cannot be dismissed but remains very low.

As described above, when considering the events that are unlikely to have occurred at this site and excluding them from the list of water-related events, the possibility of a tsunami event remains. The following sections will explore whether a tsunami could have caused the Event deposits.

3. Microfossil composition

Many charcoals are visible in the Muddy Event deposits. Similar charcoals are only found in the upper part of Paleosol (Ps), (Bp) and (Dp) (Fig. 6), indicating that the Event deposits contain surface erosion materials from that time. The Event deposits and Paleosol can be further subdivided into fine grains of palynodebris. Their compositions are depicted in Fig. 12a. The composition of the palynodebris in the Paleosol (KS-Dp) is predominantly microcharcoal, with no pollen. This is similar to the characteristics of the A horizon of the buried Holocene soil (Yamanoi, 2002, 2005). The lower KS-Bp is considered to be the B horizon of the soil from that time, and the absence of microcharcoal is common in Pleistocene loamy soils (Yamanoi, 1996). However, the occurrence of the Black Rod and its high rate are unique and unprecedented. The palynodebris of the Event deposit exhibits a low rate of palynomorphs such as pollen, similar to that of the Paleosol and general old soils. Furthermore, the high abundance of the Black Rods in the Muddy Event layer strongly suggests that the Event deposits are erosion products originating from the underlying Paleosol. Additionally, even though the Muddy Event deposit is hydrogenous sediment, it lacks palynomorphs such as pollen, confirming that the Muddy Event deposits do not resemble palynomorph-rich sediments typically found in lacustrine or fluvial muddy deposits. Among these palynomorphs, the pollen content is not substantial enough to serve as a facies fossil. Nevertheless, it's worth noting the occurrence of *Concentricystes*, which has a characteristic spiral-patterned surface structure, as an acritarch (Fig. 11b).

Concentricystes is considered an indicator species of terrestrial freshwater environments (e.g., Scott, 1992; Grenfell, 1995, etc.) since it is primarily found in lake sediments in various regions worldwide, although its taxonomic classification remains unknown. The ecology of this genus appears to be restricted to lakes and wetlands based on an analysis of the production environment of *Concentricystes* in various regions of China (32 sites) (Tang et al., 2013). While *Concentricystes* is not present in the Paleosol (KS-Dp, Bp) at this site, a small number of *Concentricystes* are identified in all

Muddy Event deposits (Fig. 12a). Despite the Muddy Event deposits mainly originating from the lower Paleosol, as described earlier, the presence of *Concentricystes* suggests that they also include deposits from lowland shallow freshwater environments outside the Paleosol.

Next, microfossils such as diatoms could not be identified using standard analytical methods. Therefore, we employed a method of separating siliceous fossils based on differences in specific gravity, which resulted in the discovery of siliceous fossil fragments depicted in Fig. 11(c-e). These fragments appear to be diatoms (Centrales) or radiolarians (Fig. 11c) and possibly sponge spicules (Fig. 11d, e). The fact that all of these fossils have a marine origin supports the hypothesis that the event involved a flow from the sea. However, marine microfossils are scarce and may be derived from Neogene sediments. The marine Neogene formation is exposed in the valley upstream of Mt. Chokai (Ozawa et al., 1982). Nonetheless, as previously mentioned, it is unlikely that the Event deposits were formed by water flow from the upper slopes, making it improbable that secondary fossils from the hinterland slopes were mixed into the Event deposits. Another possible source of derived fossils could be the Paleosol just beneath the Event deposits. However, we consider the probability of this scenario to be extremely low.

These marine microfossils and freshwater *Concentricystes* are more likely to have been transported from the seaward or the Small valley side of the lowlands, as discussed above, rather than from the upper slopes.

4. Mineral composition

The mineral composition of the Event layer reflects the composition of erosion sites during water transport. As previously mentioned, Event deposits primarily consist of eroded Paleosol deposits. Therefore, the mineral composition of the Event deposits, combined with the eroded materials, will help determine whether the water flow was toward the sea or inland. Samples for mineral analysis were collected from five horizons (KS-1 to 4, ys2) (Figs. 5, 9), two horizons of Paleosol (KS-Dp, Bp) (Fig. 5), Lapilli tuff (KS-Vs) (Fig. 4), and the current Beach sand (KS-Bs) (Fig. 2) near the study site. Since there is no evidence of Chokai volcano ejecta distribution in the beach area of this region (Ozawa et al., 1982), we assume that the beach remained unchanged, composed of minerals similar to those in the present beach sand. On the other hand, samples from the landward side of Mt. Chokai are represented by the Lapilli tuff. The volcano has been in Stage III (20,000 years to the present) of Chokai volcanic activity, mainly active in the crater on the Akita Prefecture side (Hayashi and Yamamoto, 2008). The Lapilli tuff is believed to have been widely distributed on the back slope at that time as the most recent Chokai volcanic ejecta before the formation of the Event deposits. The results are presented in Fig. 13.

The main minerals common to Event deposits and Paleosol are volcanic glass for all particles, and orthopyroxene and hornblende for heavy minerals. Specifically, the refractive index mode of volcanic glass aligns with that of Paleosol's two horizons (KS-Dp, Bp) and the lower two horizons of Event deposits (KS-1, 2), all of which are 1.502. This indicates that the lower Event layer contains particles from the Paleosol.

The mineral of particular significance is biotite. Chokai volcano has experienced recurrent volcanic activity since 0.6 million years ago. The lava primarily consists of andesite, with some basalt (Hayashi and Aoki, 1985). Biotite is not found in such Chokai volcanic ejecta. The heavy mineral composition of Lapilli tuff (Ks-Vs) also supports this (Fig. 13). Conversely, biotite is the primary heavy mineral in the beach sand (Fig. 13). The predominance of biotite among the

heavy minerals in the Event deposits raises the possibility that the water flow during the Event originated from the sea.

5. Sedimentary facies

The sedimentary facies of the Event deposits at each section are illustrated in Fig. 14. If the Event layer at this site was caused by a tsunami, the sedimentary facies would indicate the movement of tsunami water masses. In essence, the water flow in one tsunami cycle consists of a run-up flow and a backwash flow. We will now examine whether the sedimentary facies of the Event layer exhibit such distinctive features of tsunami-related water movement.

5.1 Lower facies

Typically, large tsunamis erode the land surface as they advance up the coast (Fujiwara, 2015, etc.). On Okushiri Island, clear erosion marks are visible at the base of the Event layer, believed to have been caused by past tsunamis (Kase et al., 2016). These clear basal contacts in tsunami deposits are a common feature found in contemporary tsunami deposits (Peters and Jaffe, 2010; Szczuciński et al., 2012b). The basal contact of the Event deposits at this site clearly exhibits evidence of land surface erosion during that time. The base of the Event layer extends to (Bp) in the Lower section, the lower to middle levels of (Dp) in the Middle section, and the upper levels of (Dp) in the Higher section (Figs. 5 and 14). This indicates that Paleosol erosion occurred prior to the deposition of the Event layer, with erosion depths exceeding 20 cm in the Lower section, 20-5 cm in the Middle section, and 5-0 cm in the Upper section (Figs. 5, 14). The cross-sectional shape of the basal contact is smooth in the Lower section, while it exhibits more variation in the Middle and Higher sections (Fig. 5). These concave scars in the Middle and Higher sections are considered erosional marks. Since erosion caused by running water typically deepens on the upstream side, the erosion scars are asymmetrical, with their axes tilted in the direction of the flow. The tilt angle of the erosional marks tends to incline upward in the Middle section (Fig. 7b left), while it lacks a distinct concentration in a specific direction in the Higher section (Fig. 7b right). In other words, the erosional marks in the Higher section are less likely to exhibit a consistent directional shape due to weaker erosive forces, while those in the Middle section reflect the upward component of water flow (Fig. 5C). Thus, the water flow prior to the deposition

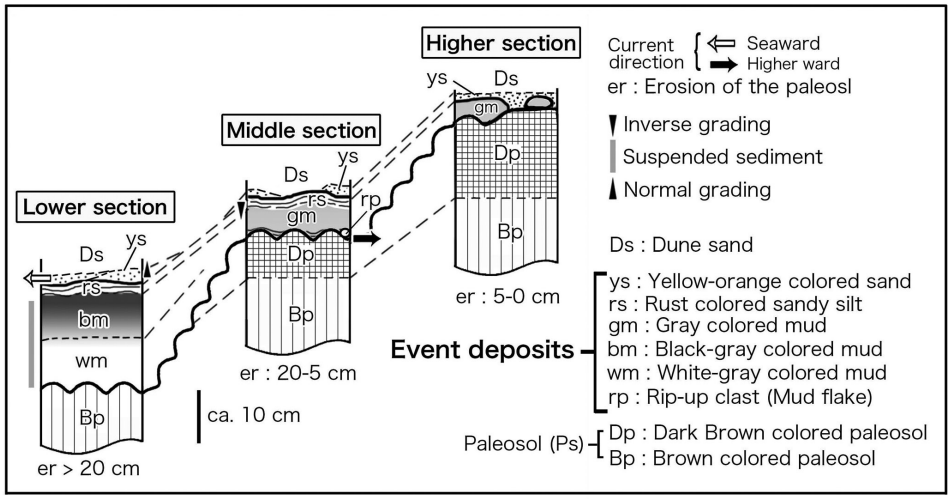

Fig. 14. Schematic transverse section of the Event deposits showing various facies and their changes on the different sections of the slope.

of the Event layer was directed landward, signifying a run-up flow in the early stage of the Event.

The next aspect to consider is the lowest part of the Event layer. In general, evidence of tsunami erosion in lower layers includes rip-up clasts, indicating a high-energy run-up flow that has not been active long enough for the gravel to become finer, similar to storm surges (Peters and Jaffe, 2010). In the lower (gm) part of the Event layer, mud flakes are often observed, especially at the bottom of concavities with widths exceeding 20 cm. However, they are rip-up clasts since they share the same homogeneity with the lower layer (Figs. 5C, 6). Rip-up clasts are found only in the Middle section. As some of the rip-up clasts are not completely separated from the sublayer (Fig. 6), it is considered that deposition began immediately after the erosion.

5.2 Middle facies

A significant portion of this Event layer consists of muddy sediments. We focus on the "white-black layer differentiation" area, where the morphological distinctions are particularly pronounced. The black part (bm) contains a higher concentration of organic matter, mainly micro charcoal, compared to the white part (wm) (Figs. 5A1 and A2). The black color is attributed to micro charcoal. Since the sedimentary particles here can be broadly classified into organic matter (with a density less than 2 g/cm^3) and inorganic matter such as felsic mineral particles (with a density around 2.7 g/cm^3), the difference in sedimentation rate between the two is believed to be responsible for the white-black layer differentiation. In other words, Stokes's law is expected to govern the deposition of muddy particles. If this is the case, the muddy Event layer can be interpreted as sediment suspended in stagnant flow.

5.3 Upper facies

The uppermost sediments of the Muddy Event deposits consist of rust-colored sandy silt (rs). The rust color results from secondary iron oxide formation. The parallel laminae of mud and sand transition into a sandy layer in the upper part of (Gm), where inverse grading is observed (Fig. 5B3). These depositions are believed to represent a shift in current dynamics from suspension to traction.

At the highest point of the Event deposits lies the yellow-orange colored sand (ys), clearly demarcated from the (rs). The sedimentary mechanism of this layer is not definitively understood on the southern side. However, at the trench location on the northern side, the (ys) layer is well developed (Fig. 9). The (ys) here is interpreted as a small fan-delta deposited by slow seaward water flow since the units from the lower (ys1) to the upper (ys3) overlap each other in a landward-to-seaward direction. Each unit of (ys) exhibits visible normal grading from sand to silty sand.

6. Is it a tsunami deposit?

The 2011 Tohoku-Oki tsunami left behind deposits in the Sendai Plain, exhibiting a variety of sedimentary facies influenced by topography. Several classifications of tsunami deposits were established based on wave transport direction and significant topographic variations (Fujiwara and Tanigawa, 2014). Notably, a three-unit structure consisting of Lower, Middle, and Upper units was observed in a relatively flat area along a hillside valley (Yamamoto Town at the southern end of the Sendai Plain) (Fig. 15b). Cross-sections featuring these multilayered structures are highly valuable as they allow us to sequentially interpret the water movement of the tsunami.

On the other hand, during the 2004 Indian Ocean tsunami, erosion and non-deposition were commonly observed in coastal areas where the tsunami made landfall, resulting in non-uniform sedimentary facies (Jaffe et al., 2006; Szczuiński et al., 2012a, etc.). However, in the southern Thailand coastal

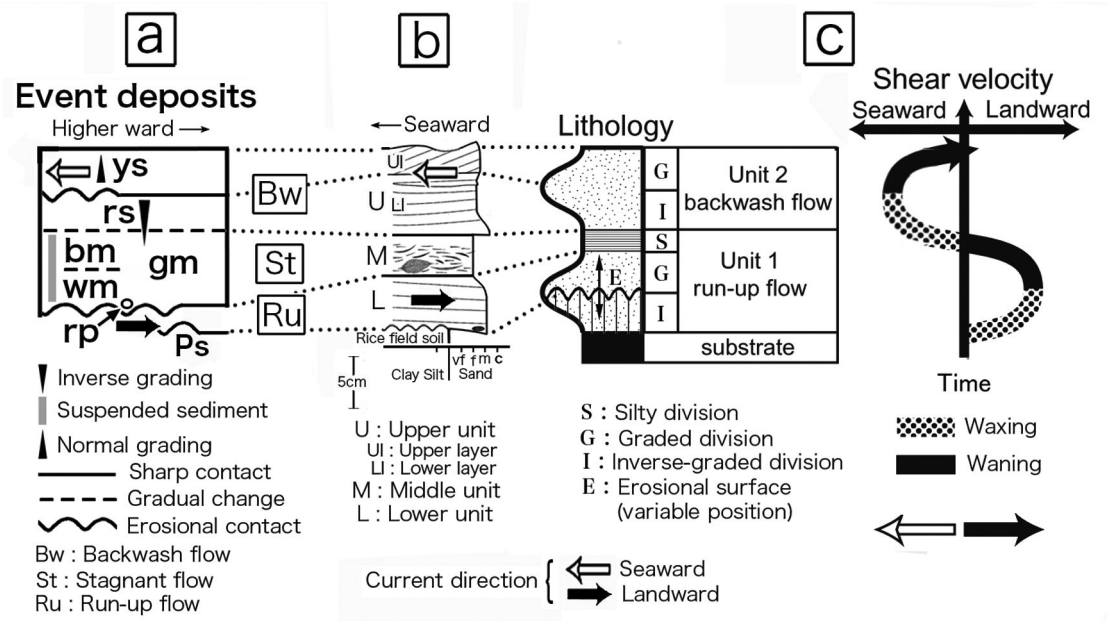

Fig. 15. Correlation with sedimentary facies of the Event deposits and present tsunami deposits.(a) Sequence of various facies of the Event deposits. For symbols of the Event deposits, see Fig.14. (b) Multiple layers were formed by the 2011 Tohoku-Oki tsunami (modified from Fujiwara and Tanigawa, 2014 and Fujiwara, 2015). (c) An ideal model of multiple deposition layers formed by a single tsunami wave from the 2014 Indian Ocean tsunami deposits (modified from Naruse et al., 2010).

flats, multiple layers of tsunami deposition have been identified. Here, ideal sedimentary facies formed sequentially, modeled based on the changes in wave velocity during run-up and backwash flows, respectively (Naruse et al., 2010). Distinguishing multi-unit deposits from the 2011 Tohoku-Oki tsunami and the tsunami layer model from the 2004 Indian Ocean tsunami from river and lake sediments relies on the presence of sedimentary facies associated with run-up flow and backwash flow. Furthermore, the presence of (S) (silt layer: stagnant facies) between the two different flow directions also reduces the likelihood of a tidal surge event. In other words, in general, if event deposits exhibit "run-up flow," "stagnant flow," and "backwash flow" in that order, it can be recognized as a tsunami deposit with a high probability of identification.

The sedimentary facies and structure of the Event deposits at each section of the outcrop slope are depicted in Fig. 14 and integrated into Fig. 15a. Although Event deposits are predominantly muddy, while recent tsunami deposits are generally sandy, it is more crucial to compare tsunami deposits formed in different topographical settings based on the direction and sequence of water flow rather than lithofacies alone. The Event deposits at this site appear to have been formed by a sequence of run-up flow (Ru), stagnant flow (St), and backwash flow (Bw), comparable to the multi-unit deposits and the tsunami layer model generated by contemporary tsunamis, as illustrated in Fig. 15 (a, b, c). Consequently, it is plausible that the Event deposits at this site may have been created by an ancient tsunami.

SUMMARY AND CONCLUSION

1. The Event layer was found in a sand mine on the foot of Mt. Chokai. The Event layer is sandwiched between Paleosol and Dune sand covering the gentle slope. The development of the Event layer is thicker in the Lower

section and thinner in the Higher section, and the highest elevation is recognized as 39.3 m. The ^{14}C age of the Event layer is about 9,000 calBP.

2.The Event deposits are hydrogenous sediment, but tsunami remains as the cause of its formation based on the elimination method from various water-related events.

3. Freshwater microfossils and some marine microfossils were observed in the Muddy Event deposits. Minerals in the Event deposits include biotite, which is abundant on the seaward beach.

4. Erosional marks at the basal contact of the Event deposits indicate that the water flow has run-up to a higher elevation. A rip-up clast is observed at the bottom of the Event deposits. In the main part of the Event deposits, there is a white-black layer differentiation, where the sediments were deposited by the suspension. The upper layer is inverse grading with lamina and becomes sandy. A fan-delta structure due to backwash flow is observed in the sand layer at the top of the Event deposits.

5. The multi-facies Event deposits at each slope correspond to the 2011 Tohoku-Oki tsunami multi-phase deposits and the tsunami layer model derived from the 2004 Indian Ocean tsunami deposits. That is, Event deposits allow run-up flow, stagnant flow, and backwash flow, which are specific to tsunami movements, in this order. Therefore, the Event deposits at this site have a possibly formed by an old tsunami.

ACKNOWLEDGMENTS

We thank the city of Nikaho, Akita Prefecture, and its Board of Education for their cooperation in the field survey and other activities. We also received permission to enter the study site from the owner of the site, Sato Forestry Co.. Drs. Kazuhiko Hori and Osamu Matsuda of Sagae Surveying and Design Office in Sagae City, Yamagata Prefecture, and Dr. Akira Kumagai of Yamagata City, Yamagata Prefecture, assisted us in the elevation survey. Mr. Yukio Toda of the Akita Prefectural Industrial Technology Center assisted us with the particle size analysis. Dr. Yukio Yanagisawa of the National Institute of Advanced Industrial Science and Technology (AIST) provided advice on microfossils. For further, two reviewers improved this manuscript. The authors would like to thank all these peoples.

REFERENCES

[Akiba et. al., 1982] Akiba, F., Yanagisawa, Y. and Ishii, T., 1982, Neogene diatom biostratigraphy of the Matsushima area and its environs, Miyagi Prefecture, Northeast Japan. *Bull Geol. Surv. Japan*, **33**, 215-239.

[Akita Pref. Education Board, 1991] Akita Pref. Education Board, 1991, Working papers of the reserve culture with the farm read construction of the Kosagawa district– The Kamikuma-Nozawa remains-. *Report of Cultural Properties in Akita Pref. No. 213*, Akita Pref. Education Board, 1- 180. *

[Atwater et al.,1995] Atwater, B., Nelson, A., Clague, J., Carver, G., Yamaguchi, D., Bobrowsky, P., … Reinhart, M., 1995, Summary of coastal geologic evidence for past great earthquakes at the Cascadia Subduction. Zone. *Earthquake Spectra*, **11**, 1-18.

[Bondevik et al., 2003] Bondevik, S., Mangerud, J., Dawson, S., Dawson, A. and Lohne, Ø., 2003, Record-breaking height for 8000-year-old tsunami in the North Atlantic. *EOS*, **84**, 289-293.

[Fujiwara, 2015] Fujiwara, O., 2015, *The Sciences of Tsunami Deposits*. Univ. Tokyo Press, 283p.

[Fujiwara and Tanigawa, 2014] Fujiwara, O., and Tanigawa, K., 2014, Bedforms record the flow conditions of the 2011 Tohoku-Oki tsunami on the Sendai Plain, northeast Japan. *Marine Geol*. **358**, 79-88.

[Goto, 2017] Goto, K., 2017, Paleotsunami researches along the Ryukyu Trench. *J. Geol. Soc. Japan*, **123**, 843-855.

[Goto et. al., 2012] Goto, K., Nishimura, Y., Sugawara, D. and Fujino, S., 2012, The Japanese tsunami deposits researches. *J. Geol. Soc. Japan*, **118**, 431-436.

[Grenfell, 1995] Grenfell, R. H., 1995, Probable fossil zygnematacean algae spore genera. *Rev. Paleobot. Palynology.* , **84,** 201-220.

[Hayashi and Aoki,1985] Hayashi, S. and Aoki, K., 1985, Petrology of Chokai volcano, northeastern Japan, Part II -Mineral chemistry-. *J. Japan Assoc. Min. Petr. Econ. Geol.* **80**, 73-82.

[Hayashi and Yamamoto, 2008] Hayashi, S. and Yamamoto, M., 2008, Chokai volcano. *J. Geol. Soc. Japan*, **114**, 87-95.

[Hirakawa, 2014] Hirakawa, K. 2014, Paleotsunami deposits along the eastern margin of the Japan Sea : The huge tsunamis recurrences and problem. *Hist. Earthq., Abstr.,* **29**, 727.*

[Ikuta et al., 2016] Ikuta, M., Niwa, M., Danhara, T., Yamashita, T., Maruyama, S., Kamataki, T., ... Hirata, T., 2016, Identification of pumice derived from historic eruption in the same volcano: case study for the Sakurajima-Bunmei tephra in the Miyazaki Plane. *J. Geol. Soc. Japan*, 122, **89**-107.

[Jaffe et al. 2006] Jaffe, B., Borrero, J., Prasetya, G., Peters, R., McAdoo, B., Gelfenbaum, G., … Yulianto, E., 2006, Northwest Sumatra and offshore island field survey after the December 2004 Indian Ocean tsunami, *Earthquake Spectra*, **22**, 105-135.

[Kase et al., 2016] Kase, Y., Nishina, K., Kawakami, G., Hayashi, K., Takashimizu, Y., Hirose, W.,... Ishimaru, S., 2016, Tsunami deposits recognized in Okushiri Island, southwestern Hokkaido, Japan. *J. Geol. Soc. Japan*, **122**, 587–602.

[Kuronuma, 1970] Kuronuma, S., 1970, *In Wadachi, K. ed. Tsunami, Typhoon Surges and Coastal Disasters*. Kyoritsu Syuppan, 245-269.*

[Minoura and Nakaya, 1991] Minoura, K. and Nakaya, S., 1991, Trace of Tsunami preserved inter-tidal lacustrine and marsh deposits: Some examples from northeast Japan. *J. Geol.,* **99**, 265-287.

[Minoura et al. 2013] Minoura, K., Hirano, S., and Yamada, T., 2013, Identification and possible recurrence of an oversized tsunami on the Pacific coast of northern Japan. *Natl. Hazards,* **68**, 631–643.

[Minoura et al. 2015] Minoura, K., Sugawara, D., Yamanoi, T. and Yamada, T., 2015, Aftereffect of subduction-zone earthquakes: potential tsunami hazards along the Japan Sea coast. *Tohoku J. Experimental Medicine.* **237**, 91-102.

[Nanayama and Shigeno, 2004, Nanayama, F. and Shigeno, K, 2004, An overview of onshore tsunami deposits in coastal lowland and our sedimentological criteria to recognize them. *Mem. Geol. Soc. Japan,* no.58, 19-33.

[Naruse et al., 2010] Naruse, H., Fujino, S., Suphawajruksakul, A. and Jarupongsakul, T. 2010, Features and formation processes of multiple deposition layers from the 2004 Indian Ocean Tsunami at Ban Nam Kem, southern Thailand. *Island Arc.* **19**, 399– 411.

[Naruse, 2006] Naruse, T., 2006, *Eolian Dust and Loess.* Asakura Publ., 197 p .*

[Naruse and Inoue, 1982] Naruse, T. and Inoue, K., 1982, Loess in North Kyushu and Yonaguni Island: Implication of aeorian dust in the Late Pleistocene. *J. Geogr. (Chigaku Zasshi),* **91**, 164-180.

[Okamura et al., 1998] Okamura, Y., Kuramoto, S. and Sato, M., 1998, Active structure and their relation to earthquakes along the eastern margin of the Japan Sea. *Bull. Geol. Surv. Japan,* **49**, 1-18.

[Ozawa et al., 1982] Ozawa, A., Ikebe, Y., Arakawa, Y., Tsuchiya, N., Satoh, H. and Kakimi, T., 1982, *Geology of the Kisakata District (Including Tobishima in the Sakata District) with Geological Sheet Map at 1:50000.*

Geol. Surv. Japan, 73p.

[Peters et al., 2007] Peters, R., Jaffe, B. and Gelfenbaum, G., 2007, Distribution and sedimentary characteristics of tsunami deposits along the Cascadia margin of western North America. *Sediment. Geol.*, **200**, 372-386.

[Peters and Jaffe, 2010] Peters, R. and Jaffe, B., 2010, Identification of tsunami deposits in the geologic record; developing criteria using recent tsunami deposits. *U.S. Geol. Surv. Open-File Rep. 2010-1239,* 39p.

[Sawai, 2012] Sawai, Y., 2012, Study on paleotsunami deposits in geologic stratum. *J. Geol. Soc. Japan*, **118**, 535-558.

[Sawai, 2017] Sawai, Y., 2017, Paleotsunami research along the Pacific coast of Tohoku region. *J. Geol. Soc. Japan*, **123**, 819-830.

[Scott, 1992] Scott, L., 1992, Environmental implications and origin of microscopic *Pseudoschizaea* Thiergart and Frantz ex R. Potonie emend. in Sediments. *J. Biogeography,* **19**, 349-354.

[Shiki, 1988,] Shiki, T., 1988, Event deposits and non-event deposits. *Chikyu Mon.*, 7, 438-440.*

[Sugawara et al., 2008] Sugawara, D., Minoura, K. and Imamura, F., 2008, Tsunamis and Tsunami sedimentology. *In* Shiki. T., Tsuji, Y., Minoura, K. and Yamazaki, T., eds., *Tsunamiites –Features and Implications*. Elsevier, Oxford, 9-49.

[Szczuciński et al., 2012a] Szczuciński, W., Kokociński, M., Rzeszewski, M., Goff, C., Cachão, M., Goto, K., and Sugawara, D. 2012a, Sediment sources and sedimentation processes of 2011 Tohoku-Oki tsunami deposits on the Sendai Plain, Japan — Insights from diatoms, nannoliths and grain size distribution. *Sediment. Geol.* **282**, 40-56.

[Szczuciński et al., 2012b] Szczuciński,W., Rachlewicz, G., Chaimanee, N., Saisuttichai, D., Tepsuwan, T. and Lorenc, S., 2012b, December 2004 tsunami deposits left in areas of various tsunami runup in coastal zone of Thailand. *Earth Planets Space,* **64**, 843-858.

[Tang et al., 2013] Tang, L. Y., Mao, L. M., Lu, X. M., Ma., Q. F., Zhou, Z. Z.,Yang, C. L., Kong Z. C. and Batten, D. J., 2013, Palaeoecological and palaeoenvironmental significance of some important spores and micro-algae in Quaternary deposits. *Chinese Sci. Bull.* **58**, 3125-3139.

[Tohno, 2000] Tohno, I., 2000, Liquefaction potential based on geological and geomorphological conditions. *Quatern. Res. (Daiyonki-Kenkyu),* **39**, 363-374.

[Yamanoi, 1996] Yamanoi, T., 1996, Geological investigations on the origin of the black soil, distributed in Japan. *J. Geol. Soc. Japan*, **102**, 526-544.

[Yamanoi, 2002] Yamanoi, T., 2002, Geologic clarifications of a landslide movement: as an example of the Tatenosawa landslide in Yamagata Prefecture, northeastern Japan. *Landslide: J. Japan Landslide Soc.*, **39**, 21-32.

[Yamanoi, 2005] Yamanoi, T., 2005, Some facies and its sequence for the sediments of landslide: As an example of the Yatsunuma landslide in Yamagata Prefecture, northeastern Japan. *J. Japan Landslide Soc.*, **42**, 17-25.

[Yamanoi, 2015] Yamanoi, T., 2015, *Soil of Japan - Geologic elucidation of the black soil and the Jomon culture-*. Tsukiji Shokan, p.249.*

[Yamanoi et al., 2016] Yamanoi, T., Tokanai, F., Kato, K., Yamada, T., Kamata, T. and Konno, S., 2016, Two tsunami deposits in the Shonai Sand Dunes, northeast Japan. *J. Geol. Soc. Japan*, **122**, 637-652.

[Yumi and Ishikawa, 2012] Yumi, M. and Ishikawa, Y., 2012, Characterization of erosional marks in the base of sediment-gravity-flow deposits: Special reference to the effect of flow duration for flute mark formation. *J. Sediment. Soc. Japan*, **71**, 173-190.

* English translations from the original written in Japanese.